Decision Support system based on machine learning to support the interpretation of ground penetrating radar images

Giuseppe Bruzzaniti[1], Giuseppe Passariello[2], Michele Passariello[3], Fabiano Rinaldi[4], Alessandro D'Apice[5], Luigi Passariello[6].

Abstract

Ground Penetrating Radar is a multidisciplinary Nondestructive Evaluation technique that requires knowledge of electromagnetic wave propagation, material properties and antenna theory. Under some circumstances this tool may require auxiliary algorithms to improve the interpretation of the collected data. Detection, location and definition of target's geometrical and physical properties with a low false alarm rate are the objectives of these signal post-processing methods. Basic approaches are focused on the first two objectives while more robust and complex techniques deal with all objectives at once. This work reviews the use of Artificial Neural Networks and Machine Learning for data interpretation of Ground Penetrating Radar surveys. We show that these computational techniques have progressed GPR forward from locating and testing to imaging and diagnosis approaches

Keywords: *Georadar, GPR, Deep Learning, Expert Systems, Decision Support Systems, Computational Networks.*

Introduction

[1] Aura Costruzioni S.r.l., Technoical Manager, giuseppe@auracostruzioni.it.
[2] Ma.Pa.COM S.rl., Data Scientist, giuseppe.passariello@mapacom.it.
[3] Ma.Pa.COM S.rl., Data Scientist, michele.passariello@mapacom.it.
[4] Centro Ricerche e Studi dei Laghi, President, fabiano.rinaldi@crslaghi.net.
[5] Ma.Pa.COM S.rl., System Engineer, alessandro.dapice@mapacom.it.
[6] Centro Ricerche e Studi dei Laghi, R&D manager, luigi.passariello@crslaghi.net.

In the field of the excavation industry, investigations using ground penetrating radar and specific software are generally used to search for underground utilities, such as metal pipes and electrical cables, to limit the risk of damage before any operation of excavation. Furthermore, it is possible to detect the presence of large rocks or archaeological finds.
Thanks to this technology it is possible to identify, with good precision and detail, a metal pipe or an electrical cable present in the first 4-5 meters of the subsoil of the site in question.
It also allows us to discriminate between the different types of pipes identified and obtain a complete reconstruction of the existing underground service networks.

Subsurface investigations with GPR Georadar
The possibility of detecting objects located underground has always fascinated man. A very attractive objective for the world of research is to develop a non-invasive exploratory technique, capable of returning images of the terrain and its composition below the topographic surface, characterized by a good degree of resolution. For this reason, the scientific community shows considerable interest in the research and innovation of geophysical techniques for subsurface exploration. Generally, we resort to the simultaneous use of different investigation techniques, and then the data obtained from direct and indirect investigations1 are compared and integrated, however this way of proceeding is not always convenient. It is very useful in the preliminary design phase of many civil works and for monitoring the state of health of hydraulic defense works, to have non-invasive investigation technologies, such as not to degrade the degrading of a work or of a piece of land during the survey. GeoRadar or Ground-Penetrating Radar (GPR) prospecting is a recent indirect investigation methodology of the subsoil, but which for example can also be used in verifying the structural integrity of civil engineering works, based on non-destructive investigation technologies. GPR exploits the phenomenon of reflection of high-frequency electromagnetic pulses generated and sent into the subsoil, allowing the measurement of the dielectric discontinuities of geo-pedological substrates. These differences are often associated with changes in water content, grain size, lithology, porosity and densification characteristics. Originally designed with the idea of investigating the most superficial portion of the soil (30-40 cm), under certain conditions, it has shown that it possesses all the requirements to be considered a valid investigation tool even for greater depths. requirements to be considered a valid investigation tool even for greater depths. One of the major advantages of GPR is that it is possible to obtain continuous recordings, not limited to a point, but rather relating to an area. Some of the advantages for which GPR is highly successful are summarized: - type of non-destructive and non-invasive investigation; - execution speed; - numerous fields of application (engineering, geology, archaeology, agronomy, environment, etc.); - versatility of the technology, the antennas can be designed and built to have specific operational characteristics such as the frequency and geometric shape of the electromagnetic field; - extreme variability in the shape and size of the object to be investigated; - wide investigation range (from a few cm to tens of metres); - cost effectiveness; - rendering of 3D images. The major disadvantage is that GPR technology is generally very dependent on the type of application to be implemented and the characteristics of the medium to be investigated.

Geophysical investigations can be divided into passive investigations, in which information is collected on already existing phenomena, and active investigations in which the responses to induced phenomena are analysed. Radar investigations are of the active type and consist of measuring the propagation time of an electromagnetic pulse sent into the ground, through which the distance to the reflecting source can be determined. This pulsation must be quite short and at the same time, the speed in the medium must be approximately constant, to allow adequate measurements. The measurement of times is of the order of magnitude of nanoseconds (10-9 s), as the depth to be investigated is limited. It is a technique very similar to reflection seismic; the difference is that the propagation of the signal depends on the property's dielectrics of the soil and not by the specific gravity. The properties are controlled primarily by the water content, in fact a variation in water content causes the reflection of part of the signalThe performance of a GPR is influenced by some factors such as dimensions, the materials used, the burial depth and orientation of the objects and the composition of the soil layers. Furthermore, there are many sources of confusion in the signal, including anomalies and sudden accidents in operational procedures, which obscure the formation of a clean target signature in the system's signal processing pipeline. One of the recent approaches to address these challenges is to leverage machine learning techniques for target detection and classification [1]. Methods based on Deep Learning (DL) are very popular as they enable image processing and understanding such as object detection, classification, etc. However, the internal inference processes of the DL model are not transparent to either the designer or user of the model. The scarcity of training data or the training procedure itself can lead to unexpected distortions in the behavior of the DL model, which may not be foreseen before the actual detection of behavioral anomalies, with even unpleasant or dramatic consequences depending on the context of use of such models. The project seeks to identify methods for applying DL to the classification of targets for GPR applications, to meet the requirements of the excavation and construction industry.

Methods

Instruments

For experimental acquisitions, a multi-frequency 200/400/800 MHz Cobra CBDwireless Georadar with a bandwidth of 50 to 1400 MHz was used.

Dataset

The dataset features is constituted by 400 radargrams, divided into two big classes:

- 100 radargrams of not anomaly acquisition
  Example:

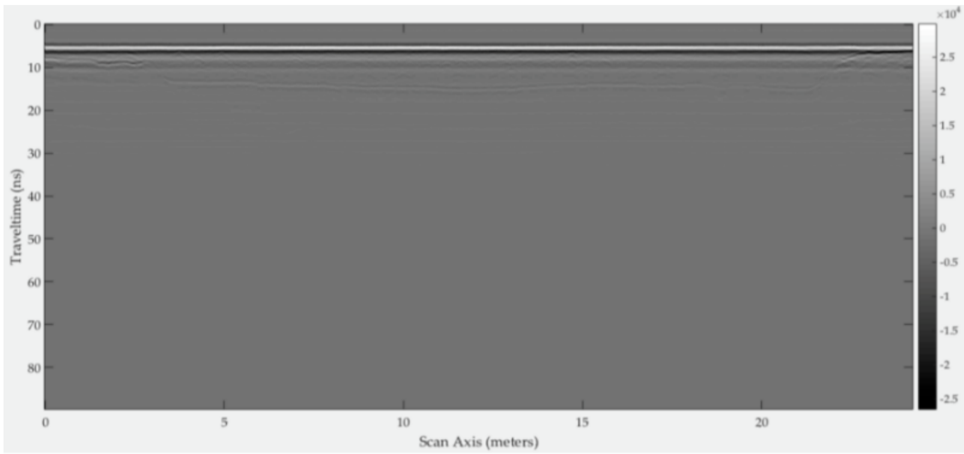

Figure 1: Image of radargram WITHOUT anomalies.

- 300 radargrams of anomaly detection
  Example:

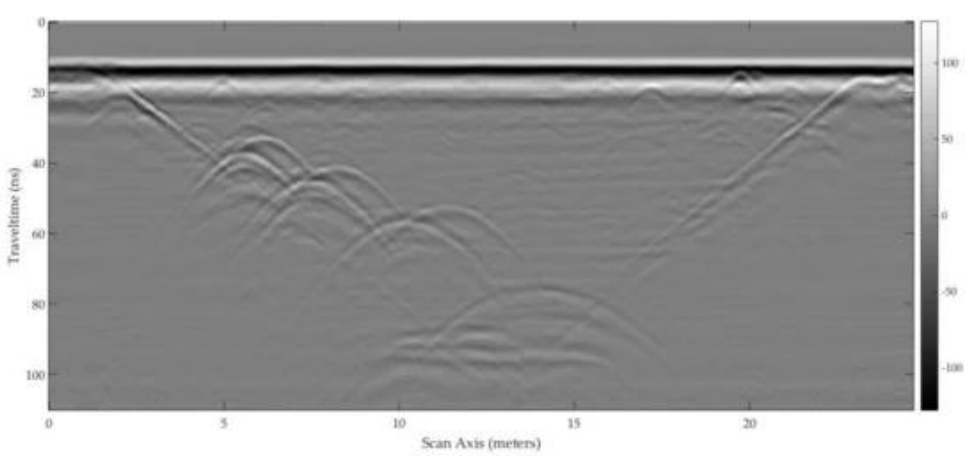

Figure 2: Image of radargram WITH anomalies.

Radargrams with anomaly detection are subdivided into six different classes of 50 radargrams corresponding to ensure knowledge of what is present underground:

Class	**Number of radargrams**
radargram of a rock	50
radargram of electrical cables	50
radargram of telephone network cables	50
radargram of gas pipes	50
radargram of various buried elements	50
radargram of various buried elements	50

Table 1: Dataset overview showing a balanced distribution of 50 radargrams per specific underground category

All images of dataset are labelled including. Each image belongs to only one radargram images category. The label of each image is saved in Training_set.csv. The Testing_set.csv contains names of radargrams in test order, which you need to predict the label and submit to Image Classifier.

Models

Authors will rely on two types of classifiers:

- binary classifier: allows you to train the system to recognize whether an abnormality is present in the radargram image or not
- multiclass classifier: it permits to train the system to recognize which type of anomaly an unknown radargram should be associated with. It should be noted that the system will recognize known anomalies and that over time for operational use it is necessary to create a much more extensive database that allows the treatment of multiple anomalies detectable through geo-radar.

Since the training dataset is ready let's create a simple CNN Model to train on the datasets of radargram images.

Results

The experimental results obtained from the training and validation phases demonstrate the high efficacy of the proposed deep learning approach for GPR radargram interpretation. Regarding the binary classification model, which was trained over 10 epochs using a dataset of 400 images (100 without anomalies and 300 with anomalies), the system achieved near-perfect performance. Specifically, for radargrams without anomalies, the precision and F1-score reached 0.99 with a recall of 0.98; similarly, radargrams with anomalies were identified with a precision of 0.99 and an F1-score of 0.98. These metrics indicate that the "light" version of the model is extremely reliable for real-time safety checks during excavation.

In the multiclass analysis, the model was trained over 50 epochs to classify six different types of underground findings, using 80% of the pre-classified images for training and the remaining 20% for validation. The results show a high level of accuracy across the categories: sewerage systems achieved the best performance with an F1-score of 0.97 and a recall of 0.98, followed by telephone networks with an F1-score of 0.90. Rocks were correctly identified with an F1-score of 0.88, while electrical cables and gas pipes showed slightly lower scores, with F1-scores of 0.86 and 0.85 respectively. Despite the increased complexity of the multiclass task, the model achieved an overall average identification rate of 88%, as confirmed by the stability of the training and validation accuracy and loss curves produced during the 50-epoch cycle.

Discussion

The areas of application of GPR (Ground Penetrating Radar) technology are currently many and of different nature: environmental analyzes and subsoil mapping, roads, tunnels and galleries, underground services, archaeology, forensic investigations. Technology allows the acquisition of detailed subsoil information or of the material under examination (radargram) without having to carry out excavations or holes and the ease, speed and reliability of this methodology explains its application in very different fields. The GPR methodology consists in the sending of variable frequency electromagnetic pulses by an antenna; these pulses propagate across the surface to be investigated and when they encounter a surface with different characteristics, a part of those electromagnetic waves is reflected towards the surface, where the receiving antenna picks them up. Ground penetrating radar equipment also allows you to measure the reflection time of electromagnetic waves, providing important information on any discontinuities present in the element under examination. The detection depth depends both on the material under examination and on the frequency of the antenna used. The low frequencies allow a greater depth of detection, and the high frequencies return a better resolution of the image of the surface investigated. For this reason, low frequencies are usually used to identify any targets in progress. In machine learning, Transfer Learning is the process of using knowledge previously acquired by solving a problem with a new (current) problem, with or without changes to the knowledge. This is possible because when a model is trained, the initial neurons of a CNN architecture extract only the high-level information, which gets narrowed down to information about the specific classes with each neural layer.
The main components GeoRadar are made up of some main components:

- transmitting system.
- receiving system.
- wave reading system.
- graphic rendering system.

Detectability of an object with GPR

The detectability of an object expresses the possibility of detecting something through electromagnetic waves; this concept therefore plays a fundamental role in the use of GPR and is sometimes mistakenly confused with resolution. A detectable object produces reflection of the incident electromagnetic signal. This capacity depends on changes in the electrical impedance of the ground and on the difference in values of the dielectric constant between the host medium and the hosted object. The amplitude of the reflected signal is expressed by the Fresnel reflection coefficient:

$$R = \frac{(\sqrt{\varepsilon_{r1}} - \sqrt{\varepsilon_{r2}})}{(\sqrt{\varepsilon_{r1}} + \sqrt{\varepsilon_{r2}})}$$

Where $\varepsilon r1$ e $\varepsilon r2$ are the dielectric constants of the ground and the hosted object respectively. The reflection coefficient takes on a positive value when $\varepsilon r1 > \varepsilon r2$, such as there is a cavity inside a dielectric. The reflectivity of a signal depends on the contrast between the dielectric permittivities on opposite faces of an interface. Furthermore, the effect that the reflected wave undergoes changes depending on the dielectric permittivity of the two materials that interface.

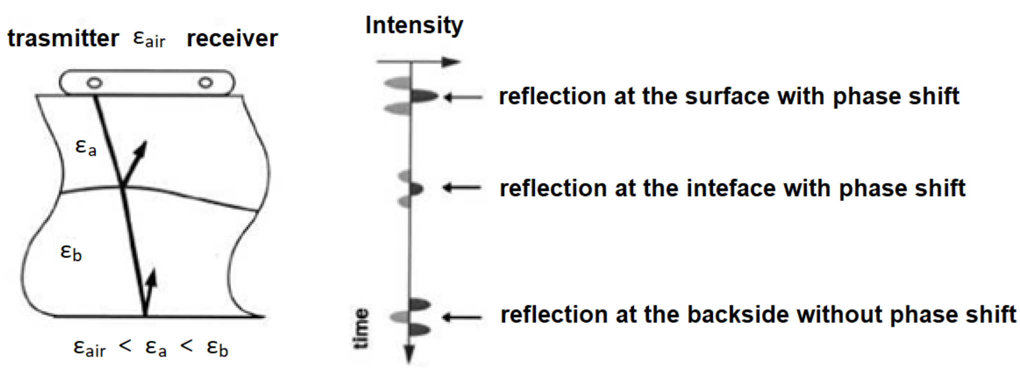

Figure 3: Reflection waves

Reflection principle for GPR.

Reflection at the interface between two different materials in which the lower one has a lower dielectric permittivity result in a phase change of the reflected signal, while if it has a higher permittivity there is no phase change [4].

Representation and interpretation of GPR sections

A section is carried out by repeating the transmission and reception cycle countless times, progressively moving the antenna along a predetermined direction. An image called a radargram is thus obtained.

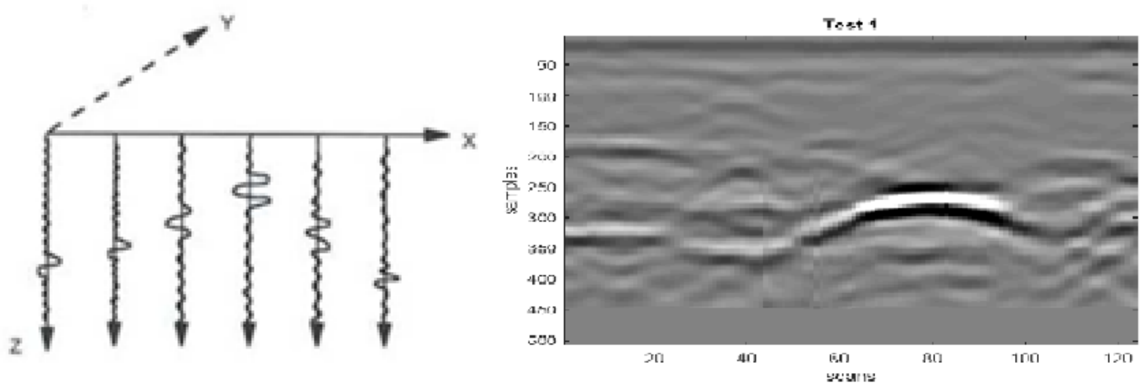

Figure 4: Schematic representation of a section and output of the processing program.

The processing program takes care of appropriately matching the traces of the received signals. The signals appear in various shades of colors (or greys), depending on their intensity. To carry out a profile there are two different operational techniques: the time domain methodology and the space domain methodology. They differ from each other in the way in which the transmission/reception cycle of the radar pulse is repeated. In time domain profiles, radar pulses are emitted at constant time intervals. In this case, the operator must move the antenna on the surface to be investigated in a specific direction, maintaining a constant speed. Only in this way will it be possible during the interpretation phase to associate the position of a reflector identified in the GPR section with the real position in the ground. In space-domain GPR sections, the interval between pulses is adjusted as a function of position. Ground penetrating radar capable of operating in the space domain makes use of a position transducer, through which the system considers the space traveled by the antenna. The emission of radar pulses is carried out whenever the system detects that the antenna, pushed by the operator, has traveled to a certain length. In this way the operator can move the antenna quickly, stop and start again without this affecting the accuracy of the section. A GPR section expresses the intensity of the pulses reflected by the substrate as a function of the arrival time and position on the surface. As already mentioned, the section is in fact the result of the juxtaposition of multiple transmission/reception cycles of radar pulses. The interpretation of the shapes resulting from the different colors of the GPR sections is a rather complex operation which must consider both the different propagation speeds of the different materials crossed, and the geometry of the investigation cone or emission cone of the electromagnetic waves sent in the ground. The geometry of this cone is like a truncated cone that opens downwards. Consequently, the radiation can also intercept targets that are not placed exactly along the vertical; their reflexes will arrive with a greater delay, following a longer journey, and will appear deeper. A typical example of this effect is the hyperbola shape shown in correspondence with small reflectors (e.g. transversally cut pipes, pebbles, small diameter cavities, tunnels, etc.), whose descending and ascending branches are the reflections recorded before and after the passage of the antenna over the vertical of the target.

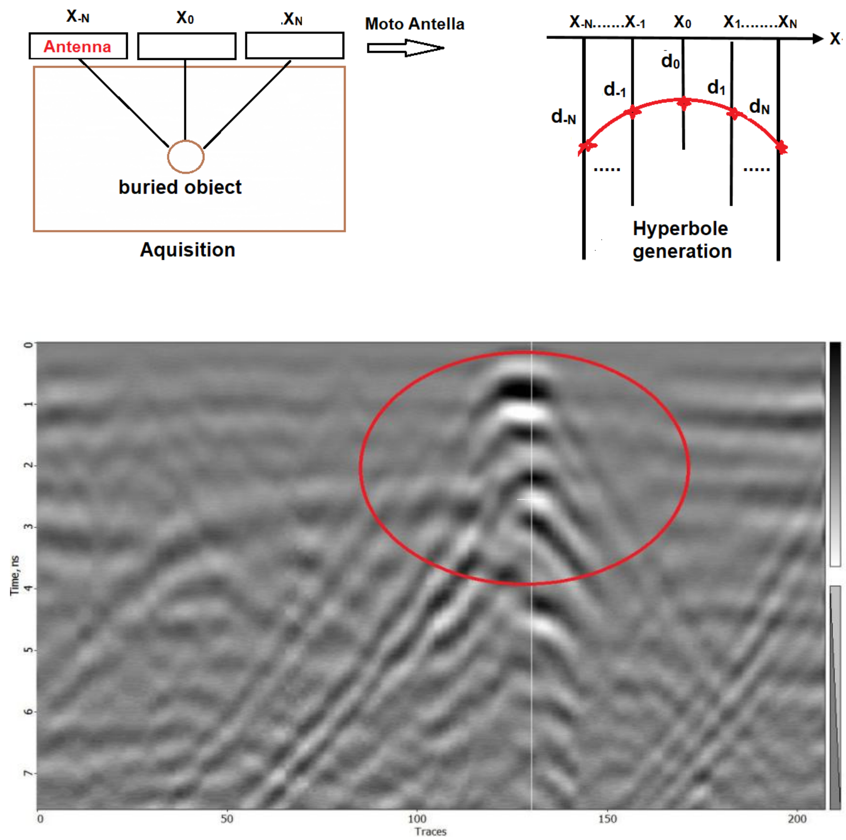

Figure 5: Examples of a GPR section for the location of underground services.

In the center of the image, the hyperbola anomaly caused by the crossing of a pipe that runs in a direction perpendicular to the section is clearly visible. Laterally extended bodies, such as large objects, stratifications or fractures, are less affected by the effect of the transmission cone and show in the profiles a shape closer to the real one. It is therefore possible with some experience to provide a sufficiently precise interpretation of the radar anomalies identified by observation of the sections alone. The interpretation of complex shape anomalies or the exact determination of the depth of the objectives requires a different approach which will be explored later.

Interpretation and processing of data

The interpretation of the shapes resulting from a radargram is a rather complex operation. There are many different factors to consider, starting from the speed of propagation of the signal in the ground, to the geometry of the target and the emission cone. The image of an object generated in a radargram does not always correspond to its geometric representation. For example, the effect of the combination of different reflectors can generate a shape in the image that does not correspond to reality, the same happens when there is a variation in the speed of propagation of the signal which can cause a dilation of the appearance of the object. The proposed solution aims to provide innovative tools based on machine learning techniques for the interpretation of radargrams in two ways:

1. Binary analysis (2 classes): aimed at automatically establishing whether the radargram shows the presence of something that can limit or create problems for excavation activities often carried out using a NO DIG machine
2. Multiclass analysis (n-classes): aimed not only at understanding the presence of "something" underground, but also at developing the ability to suggest what it could be (technological network, rock, etc.).

Both operating modes of the solution include a training and validation phase which is based on the availability of a significant number of images that can be associated with the various objects detectable during an excavation (for example; radargram of a rock, sewer radargram, radargram of electrical cables, radargram of gas pipes, radargram of telephone network cables, radargram of foundation structures, radargram of various buried elements,

This allows the creation of fairly accurate interpretative models for the automatic interpretation of radargrams. The general scheme of the solution is as follows:

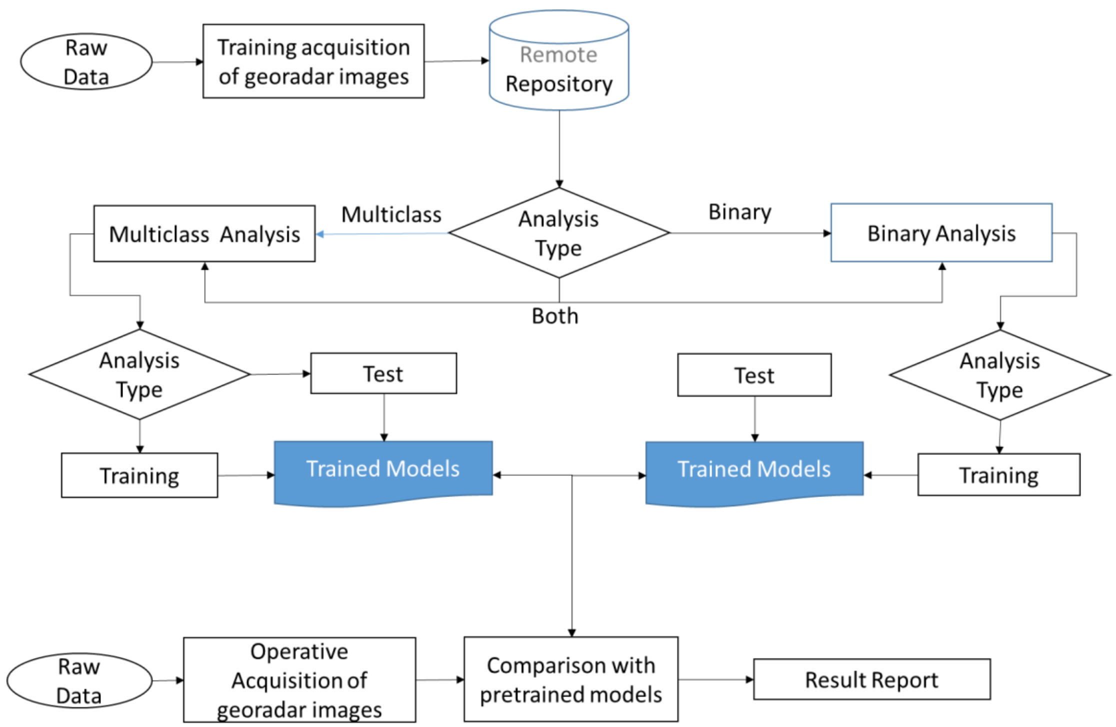

Figure 6: The DL architecture of the DSS

As a first approach we train the binary model with radargram images without anomalies (100 images) and radargram images with anomalies (300 images). We then train the model with 6 classes of which referring to findings without anomalies and 5 referring to findings with anomalies. In both cases we use a convolutional neural model:

- Convolutional Neural Network is a specialized neural network designed for visual data, such as images & videos. But CNNs also work well for non-image data (especially in NLP & text classification).
- Its concept is like that of a vanilla neural network (multilayer perceptron) – It follows the same general principle of forwarding & backward propagation.

Architecture of convolutional neural network

Components of a convolutional neural network are:

- Input image(s)-> Target images you'd like to discover patterns in-> Whatever you can take a photo (or video) of
- Input layer-> Takes in target images and preprocesses them for further layers-> input_shape = [batch_size, image_height, image_width, color_channels]
- Conlution layer-> Extracts/learns the most important features from target images-> Multiple, can create with tf.keras.layers.ConvXD (X can be multiple values)
- Hidden activation-> Adds non-linearity to learned features (non-straight lines) Usually ReLU (tf.keras.activations.relu)
- Pooling layer-> Reduces the dimensionality of learned image features Average (tf.keras.layers.AvgPool2D) or Max (tf.keras.layers.MaxPool2D)
- Fully connected layer-> Further refines learned features from convolution layers tf.keras.layers.Dense
- Output layer-> Takes learned features and outputs them in shape of target labels output_shape = [number_of_classes]
- Output activation-> Adds non-linearities to output layer tf.keras.activations.sigmoid (binary classification) or tf.keras.activations.softmax

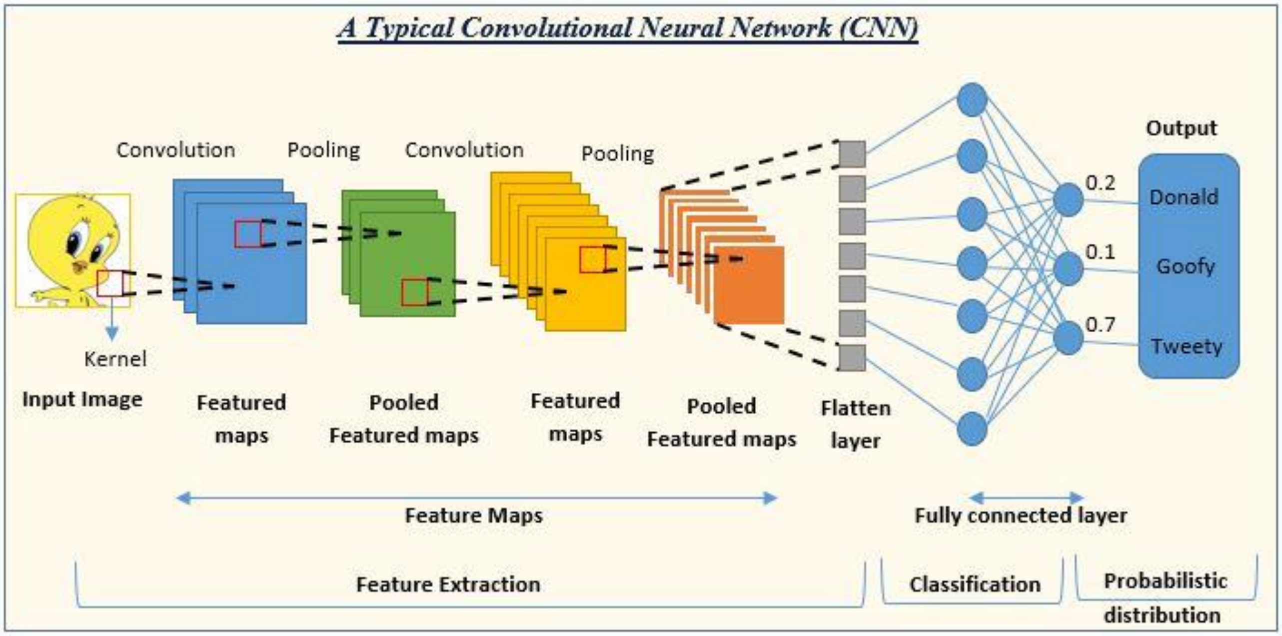

Figure 7: Convolutional Neural architecture (source credit: https://www.analyticsvidhya.com/blog/2022/01/convolutional-neural-network-an-overview/)

Mathematically, convolution is the summation of the element-wise product of 2 matrices. Let us consider an image 'X' & a filter 'Y' (More about filter will be covered later). Both, i.e. X & Y, are matrices (image X is being expressed in the state of pixels). When we convolve the image 'X' using filter 'Y', we produce the output in a matrix, say' Z'.

$$\begin{array}{|c|c|c|} \hline 1 & 2 & 3 \\ \hline 2 & 0 & 0 \\ \hline 7 & 9 & 1 \\ \hline \end{array} \quad * \quad \begin{array}{|c|c|c|} \hline 3 & 2 & 0 \\ \hline 3 & 0 & 1 \\ \hline 0 & 5 & 2 \\ \hline \end{array} \quad = \quad \begin{array}{|c|c|c|} \hline 1*3=3 & 2*2=4 & 3*0=0 \\ \hline 2*3=6 & 0*0=0 & 0*1=0 \\ \hline 7*0=0 & 9*5=45 & 1*2=2 \\ \hline \end{array}$$

Finally, we compute the sum of all the elements in 'Z' to get a scalar number, i.e. 3+4+0+6+0+0+0+45+2 = 60

We performed training with 10 epochs using 80% of the images without anomalies and with anomalies. We subsequently carried out a validation test using remaining 20% of the samples. The results are summarized in the following table:

File Type	Precision	Recall	F1-Scor
Radargramma senza anomalie	0.99	0.98	0.99
Radargram con anomalie	0.99	0.98	0.98

Table 2: Radargram recognition scores

Now we train the multiclass model on 50 epochs to teach the automatic system to correctly classify the radargram images of the 6 classes considered.

Also, in this case for training, we use 80% of the images with radargrams pre-classified during the acquisition phase and the remaining 20% of the radargram images for the validation tests. In the following graph we plot training and validation accuracy, loss and learning rate produced with training phase:

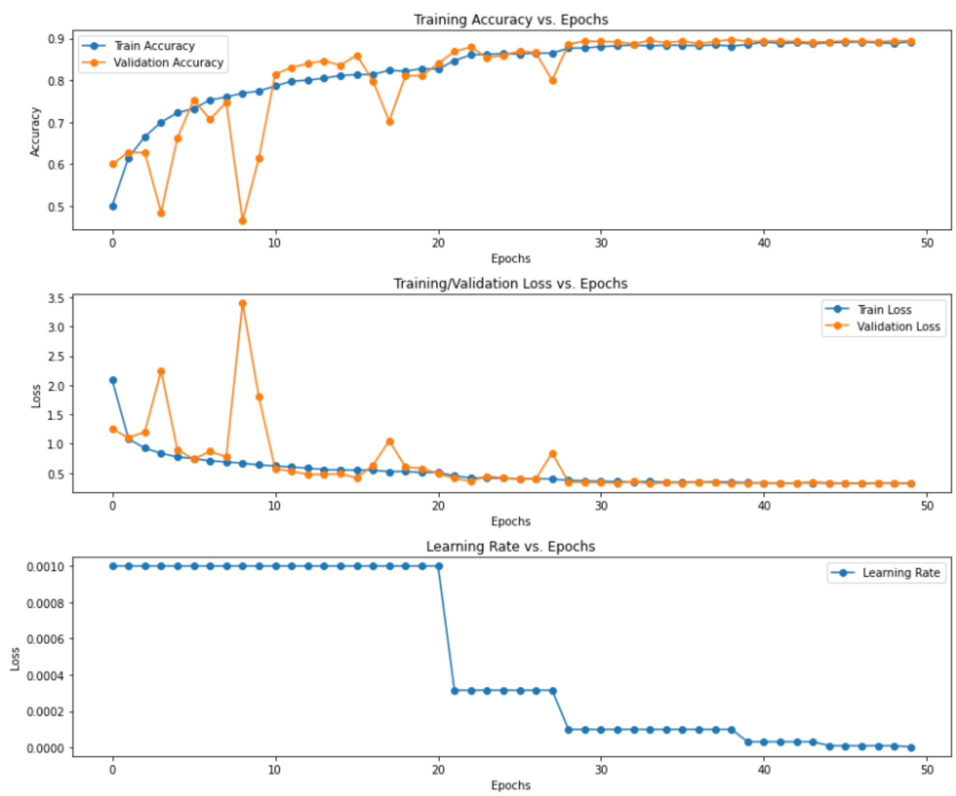

Figure 8: Training and validation accuracy, loss and learning rate produced with training phase

Result obtained at end of training and validation phases are demonstrated in following table:

File Type	Precision	Recall	F1-Score
Rock radargrams	0.86	0.91	0.88
Sewerage system radargrams	0.86	0.98	0.97
Electrical cable radargrams	0.87	0.84	0.86
Gas pipe radargrams	0.87	0.83	0.85
Sewerage system radargrams	0.91	0.92	0.92
Telephone network radargrams	0.91	0.89	0.90

Table 3: Radargram recognition scores for target class

Use cases

A possible use case of the developed decision support system can be used in reducing the pointing and drilling times of NO DIG excavators.

This is a technology that allows the laying of polyethylene, steel or ductile iron pipes along a drilled profile. The pipes that can be installed have diameters between 40 mm and 1600 mm and are used for numerous underground services (water, sewage, energy, telecommunications, etc...). The drilling profile, carefully chosen in the design phase, is followed thanks to extremely precise guidance systems, usually magnetic, such as allowing the avoidance of natural and/or artificial obstacles and the achievement of a pre-established objective, operating from a position close to the starting point. entry into the drilling ground, with a drilling machine called RIG.

There are essentially three processing phases:

- During the first phase, a pilot hole is created by introducing a column of rods into the entry point, with a drilling tool placed at the head; the phase ends with reaching the pre-established exit point;
- subsequently a suitable reamer is mounted on the drilling head which allows the diameter of the hole to be enlarged until it reaches the dimensions useful for laying the planned pipes;
- finally, the column of the pre-welded pipe is pulled into the hole, completing the work.

Drilling is usually favored using fluids - bentonite or polymeric muds -, open-air excavations along the drilling axis are not necessary and, at the end of the operations, the work area is returned to the status quo ante, through the restoration of entry and exit points. In the case of laying small pipelines, the hole boring phase can be avoided, thus reducing not only the processing times but also the dimensions of the machines used and, therefore, the construction site area. CHD (Controlled horizontal drilling) is particularly suitable for overcoming obstacles, such as rivers, canals, major roads, public areas, archaeological areas, etc. and is also used in the consolidation of landslide slopes and in the rehabilitation and containment of polluted sites. The use of this technology can be problematic in the presence of loose gravel, therefore a preliminary study of the terrain to be crossed is necessary. The design of a CHD therefore implies the execution of preliminary investigations with the aim of reconstructing the stratigraphic situation along the drilling profile and, especially in urban areas, to identify the presence of any preexisting underground services. In this sense, the possibility of examining the terrain to be crossed and knowing the correct pointing direction is certainly useful to the person in charge of horizontal excavation with the NO DIG machine. A possible use of the developed solution could be to receive real-time information from personnel moving across the territory with ground penetrating radar about the position of any obstacles to drilling to plan the route based on the indications of the DSS whose services are provided on map with survey positions appropriately georeferenced.

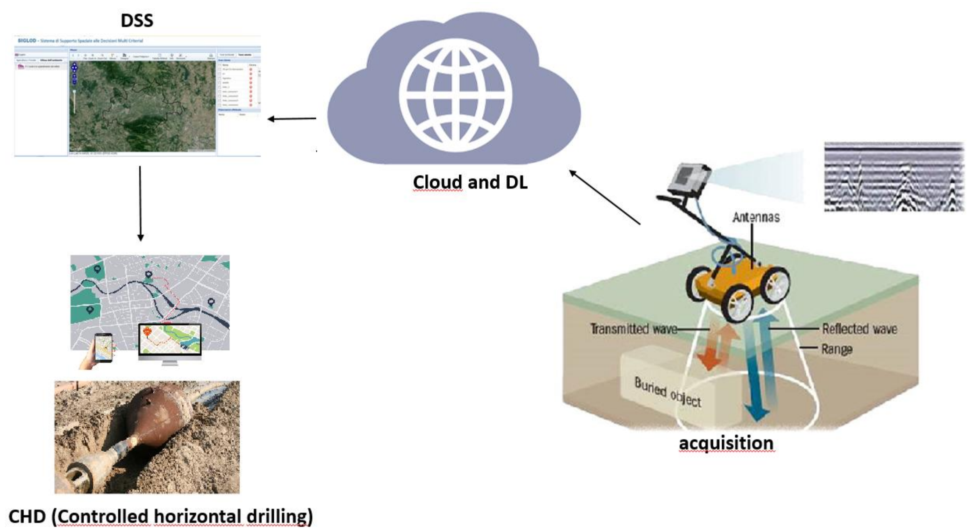

Figure 9 - training and validation accuracy, loss and learning rate produced with training phase

The software elements adopted for the development of the DSS functionalities are listed below:

<table>
<tr>
<td>

- JAVA
  - SDK (Software Development Kit) for the creation of application functions in web-oriented mode
- Spring Framework (Java framework for developing enterprise applications)
  - Web application (Spring MVC)
  - Security management (Spring Security)
  - Persistence management (Spring Data)
  - REST services (String MVC Rest)
- PostgreSQL + PostGIS
  - Databases
  - Extension for GIS
- Geoserver (Open-source server for sharing, processing and modifying geospatial data)
  - Map management
- OpenLayers (JS library for displaying

</td>
<td>

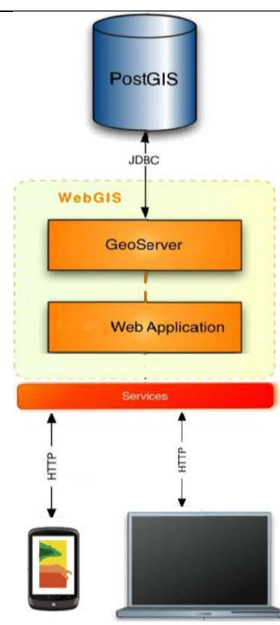

</td>
</tr>
</table>

geospatial data in web pages) • View maps ❑ Bootstrap (CSS/JS/HTML tools for creating web pages) • Web page style management	

Figure 10: Software components and their integration

Conclusion

This study demonstrates the effectiveness of integrating Machine Learning techniques for the automated interpretation of Ground Penetrating Radar (GPR) data. The proposed solution offers a dual-mode operational approach: a "light" binary classification for rapid anomaly detection and a detailed multiclass analysis for obstacle identification. The experimental results validate the robustness of the system, achieving an outstanding 99% accuracy in binary classification, which ensures a reliable safety net for identifying potential excavation hazards. Furthermore, the multiclass model reached an average identification rate of 88%, successfully distinguishing between diverse underground targets such as rocks, sewage systems, and utility networks. The integration of these models into a web-oriented DSS—leveraging Java, Spring, and PostGIS—represents a significant step toward the digitalization of the construction site. By providing real-time, georeferenced feedback, the system drastically reduces the "pointing and drilling" times for NO DIG excavators and minimizes the risk of accidental utility damage. While these scores are significant, future work will focus on expanding the training dataset to further enhance the recognition of small-diameter targets and complex soil stratigraphy, ultimately moving toward a fully autonomous subsurface diagnostic tool.

References

[1] M. Sezgin and M. N. Alpdemir. (2023) "Classification of buried objects usingdeep learning on gpr data," in Accepted for publication in 2023 6th Inter-national Conference on Advanced Systems and Emergent Technologies (IC ASET)
[2] Daniels, D. J.: (2022) Ground Penetrating Radar 2nd Edition, IET.
[3] Ni, Sheng.Huoo, Chen, Ching-Kuan and Lin, Hong-Ming (2002): Application of Ground Penetrating Radar on the void-detection in levee (Proceeding of The Twelfth (2002) International Offshore and Polar Engineering Conference).

[4] Beres, M. Jr and Haeni, F.P. (1991): Application of Ground Penetrating Radar Methods in Hydrogeologic Studies (Ground Water, Vol. 29, n. 3, PP 375- 386).

[5] Davis, J.L. and Annan, A.P.: Ground penetrating radar for high resolution mapping of soil and rock stratigraphy (Geophysical Prospecting, Vol. 37, n. 5, PP 531-551).

[6] www.gpradar.it

[7] Mellet, J. S. (1995): GPR applications in engineering, environmental management and geology (Applied Geophysics, Vol. 33, PP 157 - 166).

[8] www.malags.com

[9] Wyatt and Temples (1996): Ground Penetrating Radar detection of smallscale channels, joints and faults in the unconsolidated sediments of the Atlantic Coastal Plain (Environmental Geology, Vol. 27, n. 3, PP 219-225).

[10] Carlsten S., Johansson S., Wörman A. (1994): Radar techniques for indicating internal erosion in embankment dams (Applied Geophysics, Vol. 33, PP 157 - 166).

[11] Indagini GPR per l'individuazione della superficie piezometrica in alcune aree campione della pianura emiliana. Standardizzazione della metodologia per la pianificazione di un utilizzo a scala più vasta. Regione Emilia-Romagna.

[12] Conyers L. B. (2004): Ground-penetrating radar system technology for Archeology. Altamira Press, Walnut Creek, California.

[13] Szynkiewicz A. (2000): GPR monitoring of earthen flood banks/levees. Proceeding SPIE, Vol. 4084, 85.

[14] Biavati G., Ghirotti M., Mazzini E., Mori G., Todini E.(2008): The use of GPR for the detection of non-homogeneities in the Reno River embankments (North-Eastern Italy)., in: , 4th Canadian Conference on Geohazards: from Causes to Management, ALLISTON, ONTARIO, Canadian Geotechnical Society, 2008, pp. 1 - 9 (atti di: 4th Canadian Conference on Geohazards: from Causes to Management, Université Laval, Québec, Canada, 20-24 Mai 2008) [atti di convegno-relazione].

[15] Morris, M. (2005): Investigation of Extreme Flood Processes and Uncertainty, Project IMPACT, Final Technical Report.

[16] Gianinetto M., Lualdi M., Lechi, G. (2001): Indagini non distruttive per la diagnostica delle vie d'acqua in esercizio. possibili sviluppi sperimentali con tecniche di Telerilevamento da aereo e Georadar. International Conference "Water and Irrigation Development". 25-27 September 2001, Cremona, Italy.

[17] Md. Nazrul Islam: Embankment erosion control: Towards cheap and simple practical solutions for Bangladesh. Coastal Embankment Rehabilitation Project - South Khulshi, Chittagong, Bangladesh.

[18] www.fema.gov/hazards/damsafety

[19] Adami A. (1997): Criteri generali di progetto di un argine. La difesa idraulica del territorio, a cura di U. Maione e A. Brath, Editoriale Bios, Cosenza, PP 99-106.

[20] Covelli C., Cozzolino L., Pianese D. (2006): Sulle cause idrauliche di innesco dei fenomeni di instabilità dei rilevati arginali, XXX° Convegno di Idraulica e Costruzioni Idrauliche – IDRA 2006.

[21] Mazzini E., Simoni G.,(2008): Relazione Descrittiva: Evento di Piena del 20 maggio 2008 del Torrente Samoggia. Regione Emilia-Romagna - Servizio Tecnico Bacino Reno.

[22] Mazzini E., Simoni G.,(2008): Relazione Geologica e Geotecnica: Evento di Piena del 20 maggio 2008 del Torrente Samoggia. Regione Emilia-Romagna - Servizio Tecnico Bacino Reno.

[23] www.drcitalia.com

[24] Vianello G., Gaspari N., Gherardi M., Piana S., Rossi Pisa P., Simoni A., Bittelli M., Ventura F., Veronesi F., Antisari L.V., Zamboni N. (2006): Interventi per il ripristino ambientale dell'area Ex Fornace di Via Fiesso, Castenaso, BO. Caratterizzazione preliminare agli interventi di bonifica. Centro Sperimentale per lo Studio e l'Analisi del Suolo (CSSAS), DISTA, Università di Bologna.